Current Research in Food Science 9 (2024) 100927

Contents lists available at ScienceDirect

Current Research in Food Science

journal homepage: www.sciencedirect.com/journal/current-research-in-food-science

Understanding the characteristic changes of retrogradation behavior and edible quality of brown rice modified with inhibiting retrogradation enzymes of *Ganoderma lucidum*

Meilin Cui *, Keke Qiu, Yuchang Ma, Jiali Wang, Wei Zhao, Xiuhong Zhang **

College of food science, Shanxi Normal University, 030000, Taiyuan, China

A R T I C L E I N F O

Keywords:
Brown rice
Starch
Ganoderma lucidum
Inhibiting retrogradation enzymes
Retrogradation behavior
Edible quality

A B S T R A C T

Brown rice (BR) has gradually become a new choice for consumers due to its exceptionally nutritional value. Whereas starch retrogradation profoundly reduces its edibility, shelf-life and consumer acceptance, limiting the development of BR and even other starch-based food products. So, it is crucial for controlling the retrogradation properties of brown rice starch (BRS), and which has received significant attention in the food industry. Enzymatic modification is considered as an effective manner to retard starch retrogradation by degrading starch to an appropriate extent. *Ganoderma lucidum* can secrete various hydrolytic enzymes related to starch hydrolysis, providing a theoretical basis and feasibility for improving the starch retrogradation. Our study delves into characteristic changes of brown rice (BR) and its starch (BRS) when modified by the intracellular enzyme of *Ganoderma lucidum*, which contains several inhibiting retrogradation enzymes (*Gl*IRE), mainly including α-amylase, β-amylase, and cellulase. *Gl*IRE treatments significantly decreased the setback viscosity to 1544.33 ± 24.01 cP (2 h), diffraction intensities and relative crystallinity to 21.90 ± 0.06% (2 h) and 19.22 ± 0.19% (3 h) as per RVA and XRD analysis, accompanied with more pits and pores in surface morphology. The DSC analysis showed that *Gl*IRE treatments significantly depressed the gelatinization enthalpy to 5.86 ± 0.46 J/g (2 h) and retrogradation enthalpy. FT-IR analysis also indicated the contribution of *Gl*IRE treatments to retard starch retrogradation, including shifting the peaks of 3500 cm^{-1}-3200 cm^{-1} to lower wave numbers and decreasing the transmittance, as well as R_{1047}/R_{1022} values reducing from 0.87 to 0.73, mainly due to the shortening of starch chain length and the weakening of hydrogen bonding strength between or within the molecular chains. Simultaneously, it aslo found that *Gl*IRE treatments effectively improved the textural properties of BR, with reducing of hardness, chewiness and gumminess, and increasing of adhesiveness. Interestingly, GC-MS analysis showed that *Gl*IRE treatments could also significantly affect the types and contents of volatile compounds in BR. Our study highlights the efficacy of *Gl*IRE in starch retrogradation and rice quality-improvement, showcasing a new expansion of the research and application of *G. lucidum* and a science-based strategy for developing the edible quality of starch-based food.

1. Introduction

Rice (*Oryza sativa*) has long been one of the most extensive staple foods worldwide, especially in East-Asian countries. Brown rice (BR) is a whole grain rice composed of a bran layer, endosperm and embryo, which undergoes no or little processing after shelling. More than half of the nutrients and bioactive ingredients in BR are concentrated in the bran and germ, mainly including ferulic acid, γ-aminobutyric acid, gluten, phenols, and flavonoids (Liu et al., 2024), and showing an exceptionally nutritional value than that of white rice. Coarse-based grains, including BR, have become a new staple food choice with the development of consumers' rising demands for health.

However, one of the most significant challenges faced regarding the consumption of cooked BR is the retrogradation of gelatinized BR starch (BRS), manifesting as a decreased water retention capacity and springiness, as well as increased hardness, fragmentation and opacity of BR,

* Corresponding author. No. 339, Taiyu Road, Xiaodian District, Taiyuan, Shanxi Province, PR China
** Co-Corresponding author. No. 339, Taiyu Road, Xiaodian District, Taiyuan, Shanxi Province, PR China
E-mail addresses: cuimeilin1988@163.com (M. Cui), 1464139079@qq.com (K. Qiu), 2549890179@qq.com (Y. Ma), wangjiali816@163.com (J. Wang), 949902480@qq.com (W. Zhao), cwm_ming@163.com (X. Zhang).

https://doi.org/10.1016/j.crfs.2024.100927
Received 27 August 2024; Received in revised form 5 November 2024; Accepted 13 November 2024
Available online 15 November 2024

which finally results in reduced edibility, shelf-life and consumer acceptance, seriously limiting the practical development of BR and other starch-based food products (Niu et al., 2017). Starch retrogradation is a process of recombination and reassociation of amylose and amylopectin molecules, forming a more ordered structure after being heated in the presence of water and subsequently cooled. In general, short-term retrogradation mainly refers to the dense aggregation and crystal forming of amylose within hours (Li et al., 2022). The long-term retrogradation process mainly involves the recrystallization of the outer branched-chains of amylopectin, yielding an ordered crystalline structure after a prolonged period (Liu et al., 2019a, Liu et al., 2019b). The initial hardness and adhesiveness of processed starch-based food is attributed to the amylose retrogradation, while the long-term development of gel structure and crystallinity are related to the retrogradation of amylopectin (Wang et al., 2015). Therefore, controlling the retrogradation properties of native BRS is crucial for improving the edible quality of starch-based food products, and which is also helpful to further satisfy consumer needs and promote the development of coarse-based grains.

Various modification methods have been derived to efficiently regulate and improve the retrogradation behavior of starch, which can be classified as chemical (i.e. oxidation, cationization, acetylation, etc.) (Shah et al., 2017; Oh et al., 2019, Liu et al., 2023a), physical (high--pressure, irradiation, extrusion processing, etc) (Liu et al., 2019b, Zeng et al., 2022; Chen et al., 2023; Zhao et al., 2023), enzymatic modifications (Li et al., 2020, 2021), and complexation with other food-derived ingredients (oligopeptides, polysaccharide, quercetin, protein, etc) (Wang et al., 2015; Hu et al., 2020; Cai et al., 2023; Wan et al., 2023). In practice, the chemical modification may be detrimental to the food safety, wastewater treatment, environmental degradation, and the elevated expenses. The physical modification can be used to obtain environmentally friendly starch, without leaving chemical residues within the product or the environment, whereas some physical modification are high equipment demanding, and resulting in high production costs (Rostamabadi et al., 2024). In particular, with higher substrate selectivity, product specificity, and mild reaction conditions, higher yields, and less byproducts, enzymatic modification has been considered to produce a more optimal retrogradation effect.

Enzymatic modification can lead to degrading starch to an appropriate extent, changing the chain length, molecular size and permutation ratio of amylose and amylopectin. Maltogenic α-amylase could mainly act on side chains with a degree of polymerization of 12–24 in amylopectin and finally achieved the short-term and long-term starch retrogradation (Li et al., 2023a). A novel maltogenic α-amylase participated in the cleavage of internal starch granules, shortening its outer chains and triggering maltose formation for the inhibition of starch retrogradation (Chen et al., 2020). Transglucosidase treatment could change the average chain length, branching degree and amylose content to significantly reduce the long-term retrogradation rate of wheat starch (Li et al., 2022). The bacterial β-amylase resulted in a significant decrease in average degree of polymerization (DPn) of short chains, while fungal α-amylase caused a significant decrease in DPn of long chains for potato and arrowroot starch (Villas-Boas & Franco, 2016). Other relevant studies also showed that glucan 1,4-α-maltotriohydrolase preferred the external chains and hydrolyzed the amylopectin through exo- and endo-action causing the inhibition of amylopectin retrogradation (Wu et al., 2017). In addition, maltotetraose-forming amylase and 1,4-α-glucan branching enzyme could change the chain proportion of amylopectin and amylose content, finally reducing the rate of starch retrogradation (Li et al., 2020; Cui et al., 2024).

Ganoderma lucidum has been known as a traditional edible and medicinal mushroom for over 2000 years, which has been increasingly explored owing to its important pharmacological activities, including antitumor, anti-hyperlipidemic, cardiovascular-modulatory and anti-chemotherapy (Cui et al., 2021; Wu et al., 2024). The current research about *G. lucidum* are mainly focus on the identification of bioactive components, pharmacological function analysis, and the influence of signaling molecules on key metabolic pathways (Wu et al., 2024). Moreover, what's interesting is that *G. lucidum* could secrete various hydrolytic enzymes involved in multiple physiological metabolic pathways, including cellulase, xylanase, amylase, and ligninolytic enzyme (lignin peroxidase, manganese peroxidase and laccase), which were commonly used for digestion of cellulose, hemicellulose and lignin (Surendran et al., 2018). The existence of endocellulase, laccase and endoglucanase enzymes in *G. lucidum* also have measured and analyzed (Manavalan et al., 2015; Hu et al., 2022). Of which, the existence of these relevant enzymes of *G. lucidum,* such as cellulase, xylanase and amylase, could provide a theoretical basis and feasibility for improving the starch retrogradation.

More importantly, *G. lucidum* has been officially included in the catalog of health food ingredients in China, further demonstrating its feasibility in using *G. lucidum* or its products in food processing. In this study, the intracellular enzymes of *G. lucidum* were chosen and analyzed, which could provide a new strategy for the expansion of the research and application of *G. lucidum*, without compromising the study of its bioactive ingredients.

The objective of this study was to investigate and clarify the effect of the intracellular enzyme of *G. lucidum* on the retrogradation properties and edible quality of BR. To accomplish this purpose, we analyzed the changes in microstructure, thermal properties, gelatinization, retrogradation characteristics, texture and flavors of BR in response to enzymatic modification. We hope to provide a new approach for the research on retrogradation characteristics of starch and further expand the application scope of enzymes of *G. lucidum* in starch based staple food products.

2. Material and methods

2.1. Materials

Brown rice was purchased from Jixian Town (Shuangyashan, China). All chemicals used in this study were of reagent grade and obtained from Sigma-Aldrich Chemical Co., Ltd. (St. Louis, MO, USA) and Aladdin Biochemical Technology Co., Ltd. (Shanghai, China).

2.2. Inhibiting retrogradation enzymes of G. lucidum (GlIRE)

2.2.1. Preparation of crude enzyme solution

G. lucidum was cultivated at 28 °C for 5 d with shaking at 180 × rpm in liquid seed medium (seed medium: 10 g/L potato extract, 20 g/L glucose, 3 g/L KH_2PO_4, 1.5 g/L $MgSO_4$, 0.05 g/L VB_1, pH 5.5), then inoculated at 10% into the liquid fermentation medium at 28 °C for 4 d with shaking at 180 × rpm (fermentation medium: 20 g/L malt extract, 18 g/L yeast extract powder, 3 g/L KH_2PO_4, 1.5 g/L $MgSO_4$, 0.05 g/L VB_1, pH 5.5) (Cui et al., 2021).

The fermentation broth was centrifuged at 5000×*g* for 15 min at 4 °C and the supernatant was collected as the extracellular crude enzyme solution. Simultaneously, the mycelium was harvested and washed with distilled water, then broken by a cell ultrasonic disruptor in a mixture with phosphate buffer (1:30, pH 6.8). The homogenate was centrifuged at 5000×*g* for 15 min at 4 °C and the supernatant was immediately collected as intracellular crude enzyme solution.

2.2.2. GlIRE activities

In this study, the activities of relevant inhibiting retrogradation enzymes, including α-amylase, β-amylase and cellulase were determined. The α-amylase activity was determined following the method of Luo et al. with slight modifications (Luo et al., 2022). The crude enzyme solution (1.0 mL) was kept at 65 °C for 15 min to inactivate the β-amylase activity, then the temperature was maintained at 40 °C for 10 min. Subsequently, 1% (w/v) starch solution (1 mL) was added and reacted for 5 min at 40 °C, then DNS reagent (2 mL) was added and

boiled for 5 min. After rapid cooling, the absorbance value was measured at 540 nm and the maltose concentration was calculated. The β-amylase activity was taken as the difference between the total α+β amylase activity and the α-amylase activity.

The cellulase activity was measured using the filter paper method (Boondaeng et al., 2024). Crude enzyme solution (0.5 mL), sodium citrate (pH 4.5, 1.5 mL), and filter paper strips (50 mg) were mixed and incubated at 50 °C for 1 h, and the concentration of the released reducing sugars was measured by adding DNS reagent (1.5 mL) into the reaction mixture, which was boiled for 5 min.

2.3. BRS preparation

BRS was purified based on the method of Luo et al. with minor modifications (Luo et al., 2022). Briefly, raw BR (10 g) was steeped with 0.3% (*m/v*) NaOH (200 mL) at 40 °C for 2 h with moderate shaking, followed by standing overnight for precipitation. The supernatant was discarded while the residue was mixed with 0.3% (*m/v*) NaOH (100 mL) with stirring for 30 min, and then centrifuged at 5000×*g*. The above steps were repeated three times and the precipitate was degreased with 80% ethanol and dried at 35 °C, finally obtaining the BRS.

2.4. Sample preparation

The samples of BR (10 g) or BRS (10 g) were mixed with crude enzyme solution (40 mL) with continuous shaking (100 rpm) at 40 °C for 1, 2, 3 h, respectively, then dried at 50 °C and crushed after inactivating the enzyme. The obtained samples were named as BR-*Gl*IRE-1, BR-*Gl*IRE-2, BR-*Gl*IRE-3, and BRS-*Gl*IRE-1, BRS-*Gl*IRE-2, and BRS-*Gl*IRE-3.

Meanwhile, retrograded starch samples with a concentration of 20% *w/w* (dry basis) in water were subjected to complete gelatinization in a boiling water bath and then stored for 10 d at 4 °C. All the above samples were freeze-dried and ground (100 mesh) for further measurements.

2.4.1. Scanning electron microscopy (SEM)

The freeze-dried BRS powder was fixed on the sample table to spray gold, and the pictures were taken at an accelerating voltage of 10 kV under SEM (JSM-7500F, JEOL, Japan).

The dried BR samples were sliced up and coated with gold for observation of the surface microstructure at an accelerating voltage of 10 kV.

2.5. Analysis of retrogradation properties

2.5.1. Differential scanning calorimetry (DSC)

The gelatinization and long-term retrogradation properties were measured using DSC (NETZSCHL, Q200F3, Germany). Starch samples (3 mg) were sealed in an aluminum pan with ultra-pure water (6 mg) and equilibrated for 24 h at 4 °C. The prepared pans were heated from 40 to 130 °C at a rate of 10 °C/min under a continuous flow of dry N_2 gas. The onset, peak and conclusion temperatures (T_o, T_p and T_c) and gelatinization enthalpy (ΔH_g) were determined.

For long-term retrogradation studies, the gelatinized samples were stored at 4 °C for 5 d and 10 d, then analyzed with the same temperature profile. The retrogradation enthalpy (ΔH_r) and retrogradation ratio (R %) were calculated, of which R% was the ratio of ΔH_r to ΔH_g (Yan et al., 2021).

2.5.2. Pasting properties

The pasting properties were determined using a Rapid Visco Analyzer (RVA-TM, Sweden). The slurry with starch samples was equilibrated at 50 °C for 1 min, then heated up to 95 °C at a heating rate of 6 °C/min and held at 95 °C for 5 min. The hot sample was subsequently cooled to 50 °C at 6 °C/min and maintained at this temperature for 4 min. The paddle rotating speed was set to 960 rpm for the first 10 s to disperse the sample and then fixed at 160 rpm for the rest of the study. The pasting temperature (PaT), peak viscosity (PV), through viscosity (TV), breakdown viscosity (BV), final viscosity (FV), and setback viscosity (SV) were all evaluated (Rolandelli et al., 2024).

2.5.3. Fourier transform infrared spectroscopy (FT-IR)

The transmission spectra for the examined specimens were meticulously recorded utilizing an FT-IR instrument (Varian 660-IR, USA). The starch sample (2 mg) was mixed with fully dried 1% KBr (*w/w*, 150 mg) and analyzed at a scanning wavelength from 4000 cm^{-1} to 400 cm^{-1} at a speed of 4 cm^{-1}. The FT-IR spectra were baseline-corrected and deconvoluted by OMNIC version 8.0 software, and the absorbance ratios of 1047 cm^{-1}/1022 cm^{-1} were obtained (Lan et al., 2024).

2.5.4. X-ray diffraction (XRD)

The XRD patterns of starch samples were measured by an X-ray powder diffractometer (Ultima IV-185, Rigaku Corporation, Japan). The test conditions were adjusted, including Cu-Kα rays (wavelength 0.1542 nm), 40 kV of voltage, 40 mA of tube current, 0.02° of step size, and scanning from 10° to 30° at 2°/min. The relative crystallinity of starch was obtained to calculate the percentage of the peak area to the overall diffractogram area.

2.5.5. Raman spectroscopy

The Raman spectroscopy of starch samples was obtained by using a Laser Raman Spectrometer (InVia, Renishaw, UK), which was operated with He-Ne as the emitting light source, in the range from 200 to 4000 cm^{-1}, and at a laser wavelength of 632.5 nm. The full width at half-maximum height (FWHM) of the band at 480 cm-1 was measured.

2.6. Analysis of BR edible quality after GlIRE treatments

2.6.1. Texture analyzer

The texture of BR samples was evaluated using a texture analyzer (TAXT plus, Tengba, China) coupled with the P36R probe. In the test of raw BR samples, the pre-test, test and post-test speed were 1.0, 1.0 and 10.0 mm/s in the compression mode, respectively, and the trigger force was 10.0 g. For the cooked BR samples, the pre-test, test and post-test speed was 0.5, 0.5 and 0.5 mm/s, respectively, and the trigger force was 25.0 g.

2.6.2. Gas chromatography-mass spectrometry (GC-MS)

A gas chromatography-mass spectrometer (GC-MS 6800, Tianrui, China) was used to perform GC-MS analysis, which was equipped with a HP-5MS capillary column (60 m × 250 μm × 0.25 μm) employed for chromatographic separation. The GC program was set as follows: the carrier gas was high-purity helium with a flow rate of 1.5 mL/min, the temperature of the injection port was heated from 50 °C (held for 3 min) to 100 °C (held for 2 min) at 5 °C/min, and to 140 °C (held for 1 min) at 4 °C/min, then to 180 °C (held for 2 min) at 4 °C/min, and finally to 250 °C (held for 5 min) at 5 °C/min. The MS parameters were as follows: ion source (EI) temperature 230 °C, EI ionization source 70 eV, quadrupole temperature 150 °C, mass scanning range *m/z* 35–550 (Peng et al., 2022).

2.7. Statistical analysis

All analyses were conducted in triplicate and data were expressed as mean ± standard deviation using SPSS 24.0 software. The analysis of variance (ANOVA) was followed by Duncan's multiple-range test, and $p < 0.05$ was considered to be statistically significant.

3. Results and discussion

3.1. GlIRE activities

After fermentation for 4 days, the *Gl*IRE activities were measured

(See Fig. 1). The activities of intracellular enzymes were significantly higher than that of extracellular ones. Among them, the activity of α-amylase activity, β-amylase activity and cellulase activity could reach 69496.21 ± 1250.71, 9607.24 ± 335.73 and 75517.73 ± 2142.82 U/g, respectively. Which further verified and quantified these enzyme activities, consisting with previous studies (Surendran et al., 2018). Zhang et al. also pointed out that *G. lucidum* produced important carbohydrate-hydrolyzing enzymes, including cellulase and xylanase, which is critical to hydrolyze polysaccharides into glucose and other small molecule carbohydrates to provide nutrients for its growth and enrichment of bioactive substances, achieving high value utilization (Zhang et al., 2024). These data indicated that *G. lucidum* contained various inhibiting retrogradation enzymes and has the potential for controlling retrogradation behavior of starch. The intracellular enzyme solution was selected for further experimental study.

3.2. Morphological structure

From the SEM images of BR particles, BRS, and freeze-dried retrograded BRS with different *Gl*IRE treatments (Fig. 2), it was observed that the BR surface became increasingly rough, showing exacerbated grooves deepening with the progress of *Gl*IRE treatment time, while it did not damage the BR overall structure and further ensured its procession and consumption (Fig. 2A–D). Under 5000 × magnification, the untreated BRS granules were irregular and polyhedral in shape with a relatively smooth surface. However, after *Gl*IRE hydrolyzed treatment (1–3 h), the BRS surface was obviously eroded and rough, the number of pits and pores were increased, accompanied by more heterogeneous size, causing an overall more irregular surface morphology (Fig. 2E–H). *Gl*IRE hydrolyzed the starch granules through "surface pitting", accompanied with trimming off the external chains of the amylopectin and shortening of the starch chain length, and eventually yielding a much rougher surface (Ye et al., 2018). The decease of transmittance and the ratio of 1047/1022 cm^{-1} were also demonstrated the reducing of the short-range order of starch under *Gl*IRE hydrolysis (Fig. 3B and C), further confirming the effectiveness of *Gl*IRE hydrolysis on BRS. Studies also pointed out that after enzyme treatments (α-, β-amylase), the starch became much more irregularly shaped with leaving pocks and crevices, as well as a rougher and more porous surface, according to hydrolyzing the amorphous and the external chains of the amylopectin (Ye et al., 2018; Luo et al., 2022). Besides, upon sweet potato β-amylase treatment of starch granules, the appearance of pores and sponge-like surface erosion was observed (Vajravijayan et al., 2018). Modification by maltogenic α-amylase treatment could hydrolyze starch granules from the surface by exo-attack, followed by penetration to the inside of the granules to form visible pores and channels, also suggesting that maltogenic α-amylase could hydrolyze the α-1, 4 glycosidic bonds with exo-action state to shorten the amylopectin external chains (Liu et al., 2023b).

After retrogradation at 4 °C for 10 d, the untreated BRS were aggregated solid lumps with only few pores. In comparison, *Gl*IRE-treated BRS granules (1 h) agglomerated to a much lower extent and contained more pores, while after 2–3 h of *Gl*IRE treatments, more obvious microaggregated granules with reticular structure were produced (Fig. 2I–L), where the reticular structure were formed by dehydration during freeze-drying, suggesting the BRS captured and retained more water molecules during retrogradation process (Meng et al., 2024), which also confirmed the conclusion that *Gl*IRE treatments reduced the hardness of cooked BR (Table 1).

3.3. Retrogradation properties

3.3.1. Thermal properties

The gelatinization properties of *Gl*IRE-treated BRS and retrogradation samples were summarized in Table 1. The ΔH_g could reflect the quantity of crystallinity of the starch and measure the loss of the double-helices structure and crystalline structure of the starch (Cheng et al., 2022). *Gl*IRE treatments could significantly affect the gelatinization properties of BRS, the T_o, T_p, T_c and ΔH_g were decreased by 1.12 °C, 2.87 °C, 3.84 °C, and 2.81 J/g, respectively, after *Gl*IRE treatment of 3 h. This was likely because the structural order of BRS—mainly of double helices—was disrupted during *Gl*IRE hydrolysis, and gelatinization

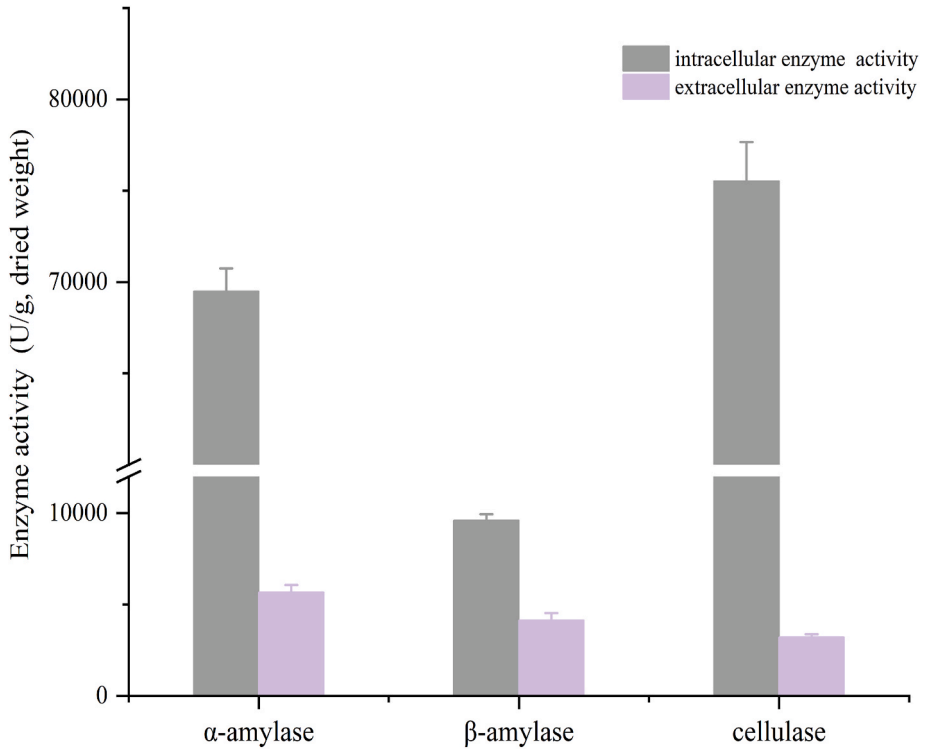

Fig. 1. The intracellular and extracellular enzyme activities of relevant inhibiting retrogradation enzymes in *G. lucidum* (*Gl*IRE).

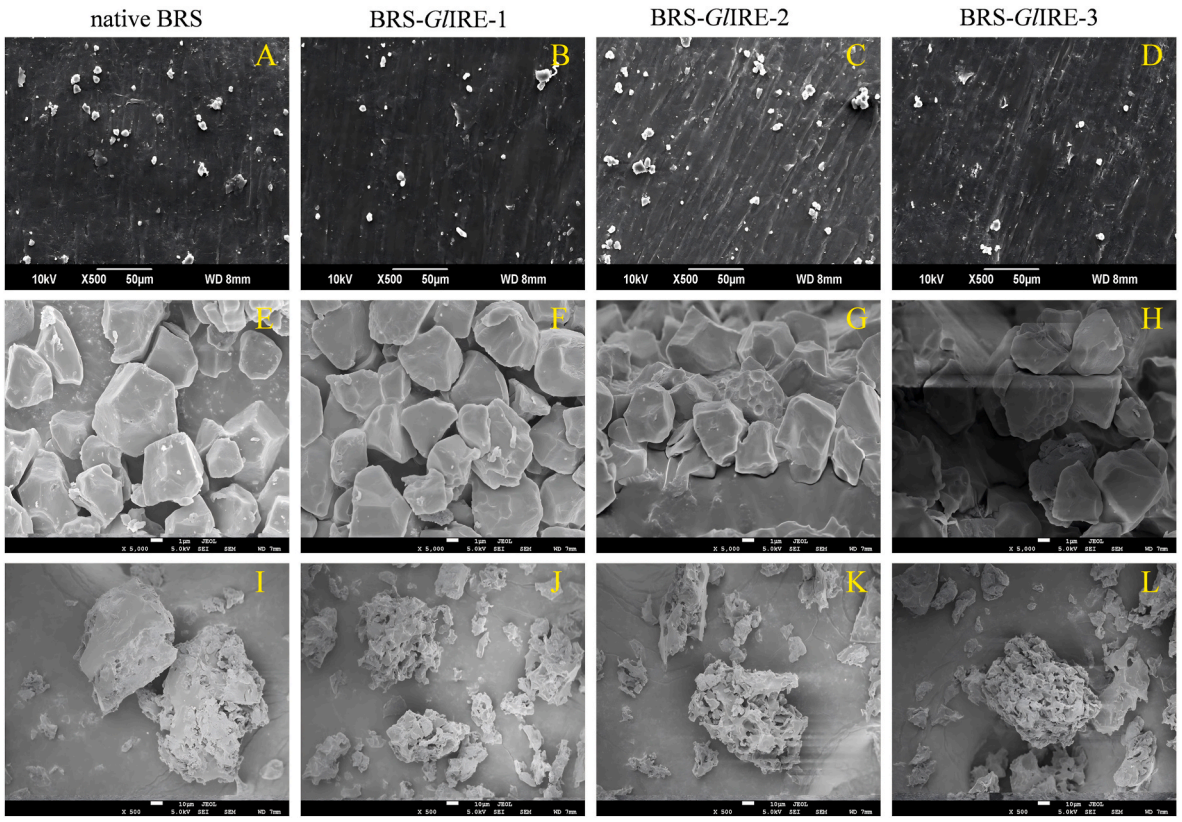

Fig. 2. SEM microstructures of BR particles (A–D), BRS (E–H) and freeze-dried retrograded BRS (I–L) with *Gl*IRE treatments for 0, 1, 2, 3 h, respectively.

enthalpy and the thermal stability was reduced (Jo et al., 2024), resulting in easier water absorption and the promotion of swelling and gelatinization at low temperature (Liu et al., 2024). Therefore, less energy was required for its gelatinization and ΔH_g showed a generally decreasing trend. Simultaneously, the relative crystallinity after *Gl*IRE treatment was significantly decreased (Fig. 3D), indicating the loss of the double-helice structure, which was also consistent with the results of structural changes measured by FT-IR (Fig. 3B and C). Shah et al. pointed out that during the treatment of β-amylase and transglucosidase, the accumulation of newly created α-1,6 branch linkages reduced the formation of junction zones between starch molecules, resulting in the destruction of the ordered crystalline structure (Shah et al., 2018). Liu et al. also found that maltogenic α-amylase treatment reduced the gelatinization temperature and ΔH_g, causing by shortening the chain length and reducing the content of double-helices (Liu et al., 2023b).

Retrogradation enthalpy (ΔH_r) represents the melting of crystalline structure by the binding of adjacent double-helices of the gelatinized starch gel during storage; higher ΔH_r is accompanied by an increased retrogradation degree of starch. After 5 and 10 days of storage at 4 °C, the ΔH_r and R% of the untreated gelatinized BRS were 5.00 ± 0.27 J/g, 61.6%, and 6.80 ± 0.35 J/g, 83.7%, respectively, indicating that the BRS is susceptible to retrogradation problems during long-term storage. The ΔH_r and R% values of *Gl*IRE-treated BRS were significantly reduced, and the ΔH_r and R% of gelatinized *Gl*IRE-BRS-2 were significantly lessened to 1.36 ± 0.22 J/g, 23.2% and 2.56 ± 0.36 J/g, 43.7%, respectively, after 5 and 10 days of storage at 4 °C. This reduction in the ΔH_r and R% of the *Gl*IRE-treated BRS suggested the inhibition of the alignment of double-helices via shortening the amylose chains and external chains of amylopectin and the formation of a less organized crystalline structure, and these structural changes were likely more conducive to controlling the long-term retrogradation of BRS (Liu et al., 2023b). Li et al. found that the cold-active 1,4-α-glucan branching enzyme hydrolysis increased the content of short-branched amylopectin (DP ≤ 10), which could not participate in stable double-helice formation, thus negatively affecting formation of the crystalline structure, and finally significantly decreasing the ΔH_r values (Li et al., 2020). Cheng et al. also observed that the β-amylase treatment regularly decreased the ΔH_r values with the increasing of treatment time, inferring that a long treatment time would change the structure of the starch branches more thoroughly, limiting the formation of recrystallization (Cheng et al., 2022). All these further demonstrated the ΔH_r and retrogradation behavior could be decrease with the increasing degree of hydrolysis of starch under enzymatic treatments, relating to the change of chain length and DPn of external chains of amylopectin (Wu et al., 2017).

3.3.2. *Pasting properties*

The pasting properties of BRS were found to be significantly affected by *Gl*IRE hydrolysis as shown in Table 2 and Fig. 3A. The PV of BRS-*Gl*IRE-3 significantly decreased to 2532 ± 141.17 as compared to native BRS, ascribed to the fact that *Gl*IRE disrupted the integrity and altered the solubility of BRS granules, as well as hydrolyzed and released more short chains, resulting in the promotion of swelling and gelatinization (Luo et al., 2022). The final viscosity values of *Gl*IRE-treated BRS were also significantly lower than those of untreated BRS, mainly caused by production of short chains inhibiting chain rearrangement in the retrogradation process (Cui et al., 2024). Previous studies pointed out that modifying α-amylase starch into soluble dextrins generally caused reduction in its PV, swelling capacity, and water-holding capacity (Wang et al., 2020). Li et al. reported that maltogenic α-amylase hydrolysis reduced the SV values, mainly reason by shortening the molecular chains and effecting molecular chains entanglement and rearrangement during retrogradation (Li et al., 2023a). The similar results of the decrease of PV and SV were likewise verified by the study of Liu et al., and explaining by the cleavage of α-1,4 glycosidic bonds to smaller oligosaccharides which were less resistant to shear force under maltogenic α-amylase hydrolysis (Liu et al., 2023b). Herein, the

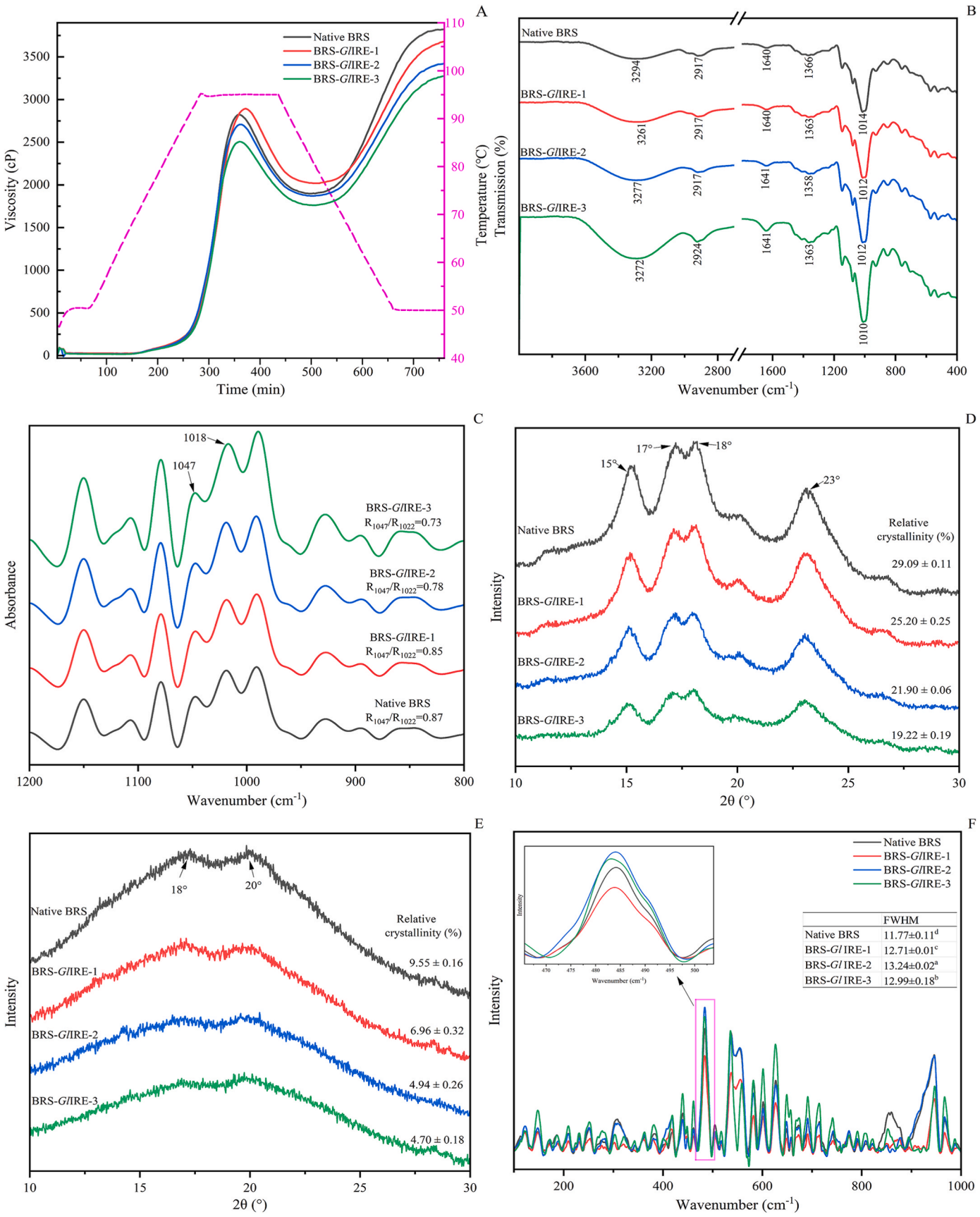

Fig. 3. Pasting profiles (A), FT-IR spectra (B), deconvoluted FT-IR spectra (C), X-ray diffraction spectroscopy (D), Raman spectra (F) of BRS with or without *Gl*IRE treatments; X-ray diffraction spectroscopy (E) of retrograded BRS with 10 days of storage with or without *Gl*IRE treatments (1–3 h).

Table 1
Thermal properties of native BRS and *Gl*IRE-treated BRS.

Samples	T_o (°C)	T_p (°C)	T_c (°C)	ΔH_g (J/g)	Ret-5days		Ret-10days	
					ΔH_r (J/g)	R%	ΔH_r (J/g)	R%
native BRS	47.44 ± 0.43^{a}	65.52 ± 0.71^{a}	83.31 ± 0.07^{a}	8.12 ± 0.18^{a}	5.00 ± 0.27^{a}	61.6	6.80 ± 0.35^{a}	83.7
BRS-GlIRE-1	46.85 ± 0.40^{ab}	64.31 ± 0.03^{b}	81.96 ± 0.11^{b}	7.12 ± 0.40^{b}	2.62 ± 0.13^{b}	36.8	3.37 ± 0.18^{b}	47.3
BRS-GlIRE-2	46.36 ± 0.27^{b}	63.62 ± 0.21^{b}	80.25 ± 0.16^{c}	5.86 ± 0.46^{c}	1.36 ± 0.22^{c}	23.2	2.56 ± 0.36^{c}	43.7
BRS-GlIRE-3	46.32 ± 0.14^{b}	62.65 ± 0.32^{c}	79.47 ± 0.25^{d}	5.31 ± 0.26^{c}	1.07 ± 0.09^{c}	20.2	2.26 ± 0.15^{c}	42.6

T_o, onset temperature; T_p, peak temperature; T_c, conclusion temperature; ΔHg, gelatinization enthalpy; ΔHr, retrogradation enthalpy. Values with different letters (a-d) in the same column were significantly different, $P < 0.05$.

Table 2
Gelatinization characteristics of native BRS and *Gl*IRE-treated BRS.

Samples	PV (cP)	TV(cP)	FV(cP)	BV(cP)	SV(cP)	PaT (°C)
native BRS	2738.33 ± 73.52^{a}	1824.66 ± 81.20^{ab}	3707 ± 95.34^{a}	913.66 ± 37.87^{a}	1882.33 ± 61.77^{a}	89.16 ± 0.48^{a}
BRS-GlIRE-1	2821.66 ± 68.01^{a}	1956.33 ± 60.74^{a}	3617.66 ± 62.29^{ab}	865.33 ± 7.57^{b}	1661.33 ± 18.71^{b}	88.25 ± 0.43^{b}
BRS-GlIRE-2	2686.66 ± 62.56^{ab}	1848.66 ± 73.10^{ab}	3393 ± 66.01^{bc}	838 ± 11^{b}	1544.33 ± 24.01^{c}	88.25 ± 0.39^{b}
BRS-GlIRE-3	2532 ± 141.17^{b}	1763.66 ± 144.50^{b}	3320 ± 201.29^{c}	768.33 ± 20.81^{c}	1556.33 ± 60.58^{c}	89.31 ± 0.49^{a}

PV, peak viscosity; TV, trough viscosity; FV, final viscosity; BV, breakdown viscosity; SV, setback viscosity; PaT, pasting temperature. Values with different letters (a-c) in the same column were significantly different, $P < 0.05$.

significant reduction in the SV values indicated the short-term retrogradation inhibition effects of *Gl*IRE treatments caused by amylose reassociation during cooling, which was in line with SEM images (Fig. 2) that *Gl*IRE-treated BRS showed more pits and pores on granular surface. BRS-*Gl*IRE-2 had the lowest SV (1544.33 ± 24.01) with a better stability and retarding-retrogradation.

3.3.3. FT-IR analysis

After gelatinization and storage at 4 °C for 10 days, the FT-IR spectra (see Fig. 3B) of native and *Gl*IRE-modified BRS displayed a wide and strong absorption peak from 3500 cm^{-1} to 3200 cm^{-1}, which could be ascribed to the classical characteristic peak of hydrophilic hydroxyl groups (-OH). Moreover, under *Gl*IRE treatments, the peaks shifted to lower wave numbers, and the transmittance gradually decreased and widened its range, indicating reduced hydrogen bonding strength among the starch molecules (Shah et al., 2018). Li et al. found that the infrared absorption peaks around 3400 cm^{-1} of the corn starch with 1, 4-α-glucan branching enzyme shifted to lower wavenumbers, demonstrating the decrease of the strength of hydrogen bonds and further retarding its long-term retrogradation (Li et al., 2016). The intense peak at about 2900 cm^{-1} was related to stretching vibrations of the -CH_2 functional group. The absorption peaks at 1650, 1370 and 1010 cm^{-1} corresponded to the bending-vibrations (or symmetric deformation-vibration) of C=O, C-H and C-O characteristic functional groups. The *Gl*IRE modification resulted in the widening of transmittance ranges of absorption peaks at 2900, 1650, 1370 and 1010 cm^{-1}. This might be attributed to the shortening of the starch chain length and the reduced spatial site resistance after *Gl*IRE modification, which weakened the strength of hydrogen bonds between or within the molecular chains and led to the irregular arrangement or deconvolution of the helical structure (Cui et al., 2024). The absorption bands at 1022 cm^{-1} and 1047 cm^{-1} are related to the amorphous structure and ordered (or crystalline) region of starch, respectively. The ratio of 1047/1022 cm^{-1} obtained from the deconvoluted FT-IR is commonly used to determine the short-range order of starch, qualifying its retrogradation behavior (Lan et al., 2024). The addition of *Gl*IRE treatments significantly reduced the R_{1047}/R_{1022} values from 0.87 to 0.73 of the refrigerated samples, eventually reducing the ordered structure of BRS during the retrogradation process (Fig. 3C). The level of starch crystallinity depended on the chain lengths of amylopectin molecules, when the chains obtained by hydrolysis were too short to form the double-helices, they formed the amorphous regions with low susceptibility, instead of arising the crystallinity of the starch (Shi et al., 2014). This decrease in intensity was in agreement with the decrease of the relative crystallinity in XRD analysis (Fig. 3D) and the reduce of ΔH_g of DSC results (Table 1). G4-amylose treatment also decreased the ratio of R_{1047}/R_{1022}, indicating that G4-amylose could effectively enter into the starch granules and destroy its ordered structures by shorting the length of amylopentin (Cui et al., 2024). A report of Ye et al. found that the treatment of the extruded starch with β-amylose decreased the R_{1047}/R_{1022} values by reducing the chain lengths and extending the amorphous regions (Ye et al., 2018). The same change of the ratio of R_{1047}/R_{1022} also appeared in the study of Guo (2018), indicating that the amorphous domain in starch increased after enzyme modification (branching enzyme, β-amylose and transglucosidase) since α-1,4-glycosidic bonds were replaced by α-1,6-glycosidic bonds.

3.3.4. XRD pattern analysis

The effects of *Gl*IRE treatments on the long-range order degree of crystallinity in BRS were determined (Fig. 3D). Native BRS showed an A-type X-ray pattern with characteristic strong diffraction peaks at 15° and 23°, double peak at 17° and 18°, and a peak of lesser intensity at 20° of 2θ angles (Liu et al., 2019a). The relative crystallinity difference might be attributed to the orientation of double-helices within the crystalline area, largely controlled by the chain lengths of the amylopectin molecules (Liang et al., 2020). Under *Gl*IRE treatments, the peak intensities were obviously weakened and the relative crystallinity of BRS was also significantly reduced. The BRS-*Gl*IRE-3 showed the lowest relative crystallinity of 19.22 ± 0.19%, which meant the destruction of its densely-packed crystalline structure and the presence of great amount of short chains. Specifically, the branch chains of amylopectin were hydrolyzed too short to rearrange and reassociate double helices, blocking the recrystallization of amylopectin (Cheng et al., 2022). Thus, the samples treated with deeper *Gl*IRE corresponded to lesser retrogradation crystals in the storage period. The previous study reported that β-amylose treatment decreased the relative crystallinity, according to converting the crystalline amylopectin region of starch into an amorphous state (Ye et al., 2018). Zhai et al. utilized maltogenic α-amylase to treat wheat starch and likewise found a reduction of relative crystallinity, indicating damage of starches at the crystalline structure level (Zhai et al., 2022).

The long-term retrogradation of native and *Gl*IRE-modified BRS with 10 days of storage was shown in Fig. 3E. The XRD patterns of BRS and BRS-*Gl*IRE were altered to two peaks at 17° and 20° of 2θ angles after gelatinization. This was attributed to the rapid molecular rearrangement of linear amylose due to small spatial site resistance during short-term

retrogradation and the recombination of outer side chains of amylopectin through hydrogen bonds and the formation of double-helices structure in long-term retrogradation (Chang et al., 2021). It could be clearly seen that *Gl*IRE treatments could obviously lower the intensity of diffraction peaks and the relative crystallinity (9.55 ± 0.16% to 4.70 ± 0.18%), suggesting that it could significantly reduce the long-term retrogradation rate of BRS, explained by the break of its long-range ordered structure and the reduced formation of double-helices and weaker development of aggregates, Which was consistent with the results of FT-IR and DSC. In the study of Li et al., the relative crystallinity were significantly decreased with transglucosidase treatment, indicating that the molecular chains of starch were cleaved to very short branch chains after hydrolysis, which wasn't easier to entangle each other to develop crystalline aggregates (Li et al., 2021).

3.3.5. Raman spectroscopy analysis

The FWHM of the band at 480 cm^{-1} in the Raman spectra is strongly associated with the short-range ordered molecular structure of starch (Wang et al., 2015); the larger FWHM, the lower the short-range ordered structure. As shown in Fig. 3F, the FWHM of BRS-*Gl*IRE was generally higher than that of native BRS at 480 cm^{-1} and increased from 11.77 ± 0.11 to 13.24 ± 0.02 (2 h), indicating the poor short-range molecular order in *Gl*IRE-treated samples. This suggested that *Gl*IRE treatments disrupted the hydrogen bones inside the starch molecules and hindered the re-formation of the helical conformation, thereby inhibiting the periodic helical arrangements during retrogradation. These results complemented the findings of DSC, FT-IR and XRD. Wang et al. found that the FWHM of chlorogenic acid-starch mixtures were generally higher than lotus seed starch, indicating the poor short-range molecular order (Wang et al., 2021). Huang et al. also proved the lower FWHM values indicating higher relative crystallinity, showing the importance of water content and heating temperature on starch retrogradation (Huang et al., 2021).

3.4. BR quality under *Gl*IRE treatments

3.4.1. Analysis of texture properties

The texture properties of BR are important indicators of its edible quality, including the firmness of raw BR, and the hardness, adhesiveness, springiness, cohesiveness, gumminess, and chewiness of cooked BR. For raw BR, *Gl*IRE treatments (2–3 h) could significantly reduce its firmness (Table 3), mainly due to the partial breakage of its surface cortex and the decomposition of internal substances, corroborating by the SEM results. Moreover, the above SEM analysis of BR particle demonstrated that the *Gl*IRE treatments didn't destroyed BR overall morphology (Fig. 2).

Hardness and adhesiveness are two main and stable indicators of consumption preferences. Previous studies have proved that the amylose content and the proportion of its intermediate to long chains have a positive correlation with hardness and a negative correlation with adhesiveness (Karim et al., 2024). In general, starch retrogradation contributes to the development of hardness and the suppression of adhesiveness. With *Gl*IRE treatments, the hardness, gumminess and chewiness of cooked BR were significantly reduced, while its adhesiveness was increased. During the cooking process, with the damage of surface cortex after *Gl*IRE hydrolysis, more amylose leaches into the surrounding water, preventing the formation of solid-like gel during short-term retrogradation (Xiong et al., 2022a). Also, more amylopectin short chains are generated by hydrolysis and reinforce the water-holding capacity, complementing the potential decrease in adhesiveness (Zhang et al., 2023). The damaged surface can also provide more water-absorbing channels and allow more water to enter the BR interior quickly during cooking, which is beneficial for gelatinization and results in a softer texture, effectively improving the flavor and quality of cooked BR.

Moreover, in the sense evaluation analysis (Tables S1 and S2), the cooked native BR had the poor edible quality, including dark yellow color, high hardness, low adhesiveness, and slightly coarse texture when chewing. With *Gl*IRE treatments (2–3 h), the indicators of flavor, adhesiveness, hardness and taste have significantly improved, as well as the total scores reaching to 78.7 ± 5.8 and 82.2 ± 6.3, respectively. The sensory quality of cooked rice was related to the water absorption during the cooking process (Ghasemi et al., 2009). After *Gl*IRE treatments, the destroyed epidermal layer enhanced water absorption capacity of BR, causing the water more easily to enter its inside structure and promoting starch pasting during cooking. Besides, the *Gl*IRE treatments could effectively retard BRS retrogradation combined with the above analysis. All these demonstrated a significant improvement in sensory quality and increase of consumer acceptance.

3.4.2. Flavor analysis

The volatile compounds in BR after *Gl*IRE treatments of 1–3 h and intracellular enzyme solution of *G. lucidum* were identified and analyzed by GC-MS. As shown in Table 4, a total of 41 volatiles were found, including 8 alcohols, 6 aldehydes, 13 esters, 2 ketones, and 12 hydrocarbons, that might contribute meaningfully to the aroma of rice. The relative percentage of the chromatographic peak area was used to represent the relative content of volatile compounds and to characterize their interactions.

Aldehydes are mainly derived from lipid oxidation and decarboxylation, contributing most to the overall flavor among all categories because of the relatively low aroma threshold. They have a fruity and sweet aroma at low concentrations, whereas increasing their concentration will produce an unpleasant order of oil oxidation (Chen et al., 2021). After *Gl*IRE treatments, the contents of hexanal, isovaleraldehyde, heptanal, nonanal, and n-octanal were increased, while their relative percentages were still low. Among them, hexanal, with grass-like flavor, is aroma-active compound playing important roles in rice flavor (Zhao et al., 2022). Meanwhile, we also found that the intracellular enzyme solution of *G. lucidum* contained various aldehydes. During the reaction with BR, most of its aldehydes were reserved in BR and showed an increasing trend with the increase of reaction time. In particular, the enhancement of hexanal content could further improve the BR flavor, which was more attractive to consumers.

Alcohols, as the second abundant volatiles in cooked rice after aldehydes (Guan & Zhang, 2022), usually render rice a softer, sweet, floral and fruity aroma. After *Gl*IRE treatments, the relative contents of 1-octene-3-ol and ethanol increased, while those of 2-heptanol, eucalyptol, dimethylsilanediol, and 4-terpinenol reduced. Notably, 1-octene-3-ol has the odor of mushroom and vanilla, and it plays a major role in

Table 3
Texture parameters of native BR and *Gl*IRE-treated BR.

Samples	Uncooked	Cooked					
	Firmness/g	Hardness/g	Adhesiveness/ (g.s)	Springiness	Cohesiveness	Gumminess	Chewiness
naive BR	13787.47 ± 702.29^{a}	1234.81 ± 46.39^{a}	−38.11 ± 1.70^{a}	1.83 ± 0.19^{a}	0.65 ± 0.07^{a}	806.69 ± 96.57^{a}	1466.19 ± 140.51^{a}
BR-GlIRE-1	12900.26 ± 897.53^{a}	1162.41 ± 90.21^{a}	−46.20 ± 1.09^{b}	1.33 ± 0.06^{b}	0.66 ± 0.05^{a}	764.70 ± 32.67^{ab}	1014.51 ± 55.85^{b}
BR-GlIRE-2	10484.40 ± 1328.68^{b}	1022.55 ± 37.41^{b}	−58.11 ± 1.40^{c}	1.40 ± 0.05^{b}	0.67 ± 0.03^{a}	682.51 ± 27.06^{bc}	958.03 ± 59.79^{b}
BR-GlIRE-3	10957.14 ± 973.42^{b}	957.45 ± 70.33^{b}	−67.89 ± 0.64^{d}	1.31 ± 0.15^{b}	0.64 ± 0.04^{a}	609.71 ± 67.43^{c}	799.35 ± 178.95^{b}

Values with different letters (a-d) in the same column were significantly different, $P < 0.05$.

Table 4
Flavor profiles of native BR, *Gl*IRE-treated BR and intracellular enzyme solution of *G. lucidum*.

Flavor substances		CAS	Relative content (%)				
			naive BR	BR-*Gl*IRE-1	BR-*Gl*IRE-2	BR-*Gl*IRE-3	Intracellular enzyme solution of *G. lucidum*
Alcohols	2-Heptanol	543-49-7	0.68	–	–	–	–
	Eucalyptol	470-82-6	0.34	0.08	–	–	–
	Dimethyl-silanediol	1066-42-8	2.24	1.10	0.71	0.86	0.62
	4-Terpineol	562-74-3	0.54	0.13	0.26	0.33	0.14
	3,4-Dihydroxyphenylglycol	56114-62-6	1.48	1.05	1.07	1.33	–
	1-Octen-3-ol	3391-86-4	–	1.14	0.89	1.70	3.49
	Ethanol	64-17-5	–	0.13	0.15	0.24	0.16
	Isopentanol	123-51-3	–	–	–	0.24	–
Aldehydes	Hexanal	66-25-1	1.24	2.22	1.99	3.29	3.31
	Ethyl vanillin	121-32-4	0.80	0.27	–	–	–
	Isovaleraldehyde	590-86-3	–	0.38	0.58	1.30	6.16
	Heptanal	111-71-7	–	0.56	0.67	0.51	0.59
	n-Octanal	124-13-0	–	–	0.41	0.45	0.50
	Nonanal	124-19-6	–	0.29	0.27	0.42	0.21
Esters	Methyl myristate	124-10-7	0.09	0.14	0.20	0.27	0.53
	Methyl caproate	106-70-7	0.48	0.88	1.11	1.94	0.10
	Arsenous acid tris ester	55429-29-3	0.39	–	–	–	–
	Acetic acid methyl ester	79-20-9	–	–	0.56	0.88	–
	Heptanoic acid methyl ester	106-73-0	–	0.11	0.23	0.19	–
	Octanoic acid methyl ester	111-11-5	0.21	–	0.29	0.47	0.28
	Nonanoic acid methyl ester	1731-84-6	–	0.11	0.09	0.14	–
	Benzoic acid methyl ester	93-58-3	–	–	0.21	0.49	–
	Methyl phenylacetate	101-41-7	0.19	0.24	0.21	0.30	0.17
	Isoamyl phenylacetate	102-19-2	1.50	2.60	1.53	3.19	17.70
	Methyl palmitate	112-39-0	1.22	1.41	1.90	2.50	2.80
	Methyl linoleate	112-63-0	0.45	0.42	0.49	0.55	–
	Methyl elaidate	1937-62-8	0.60	0.55	0.64	0.79	–
Ketones	Heptan-2-one	110-43-0	0.11	0.14	0.10	0.17	0.05
	3-Octanone	106-68-3	–	–	0.29	0.38	0.16
Hydrocarbons	p-Xylene	106-42-3	0.52	2.08	2.77	1.21	–
	Decane	124-18-5	0.60	0.66	0.42	0.48	–
	p-Cymene	99-87-6	0.39	0.12	–	–	0.14
	Limonene	138-86-3	0.68	0.42	0.30	0.24	0.20
	Styrene	100-42-5	0.23	–	1.29	0.33	–
	Decamethyl-cyclopentasiloxane	541-02-6	23.59	28.36	28.06	24.83	10.54
	9-methylheptadecane	26741-18-4	0.17	0.19	–	0.13	–
	Dodecane	112-40-3	0.17	0.19	0.15	0.23	–
	Dodecamethyl-cyclohexasiloxane	540-97-6	0.24	–	0.10	0.08	0.14
	Tetradecamethyl-cycloheptasiloxane	107-50-6	8.19	6.31	6.51	6.44	10.50
	Octadecamethyl- cyclononasiloxane	556-71-8	0.49	0.39	0.34	0.37	0.24
	Eicosamethyl-cyclodecasiloxane	18772-36-6	0.24	–	0.11	0.15	–

rice flavor with a low concentration threshold (Sansenya et al., 2018). Combined with the results of Tables 4 and it also could tentatively assume that the increase content of 1-octene-3-ol in BR was mainly due to the retention of the intracellular enzyme solution of *G. lucidum*. While the relative content of some alcohols (i.e. 2-heptanol, eucalypyol, dimethyl-silanediol, etc) decreased, this result may be explained by alcohols interaction with starch and proteins via hydrogen bonds and hydrophobic interactions, and some branched starch disintegrated after *Gl*IRE treatments, which caused alcohols to volatilize (Wang et al., 2023).

Esters usually present a fuller, sweet and fruity flavor. After *Gl*IRE treatments, the types and contents of the majority of identified esters significantly increased, contributing to more volatiles in rice. The increase of the relative contents of some esters (such as methyl myristate, isoamyl phenylacetate, methyl palmitate) could be tentatively attribution to the retention of the intracellular enzyme solution of *G. lucidum*. The intracellular enzyme solution of *G. lucidum* was a multi-enzymatic system, there were also a variety of other enzymes (i.e. proteases, lipases, etc) (Xiong et al., 2022b; Cen et al., 2024), causing the chemical reactions about the degradation of fatty acids and protein decomposition and transformation in the bran cortex, and ultimately resulting in changes in flavor components, which mainly concerned to the increase of the relative contents of some methyl esters, methyl caproate and p-Xylene. Most hydrocarbons have relatively high odor thresholds and no flavor characteristics. These were also affected by enzymatic hydrolysis, and even though some of them had high contents, this did not significantly influence the aroma of rice (Li et al., 2023b), which mainly played a synergistic role with the alcohols.

To summarize the above analysis, the new generation or content change (increase or decrease) of volatile compounds under *Gl*IRE treatments were mainly caused by two reasons: (i) the retention of flavor substances in the enzyme solution of *G. lucidum*; (ii) chemical reactions under enzyme treatments, including the degradation of fatty acids and protein decomposition and transformation in the bran cortex. In other words, *Gl*IRE treatments could significantly affect the types and contents of volatile compounds, contributing to the improvement of rice flavor.

4. Conclusions

This study investigated the retrogradation behaviors of BRS and the quality of BR treated with *Gl*IRE. After *Gl*IRE treatments, the morphological structure of BRS changed significantly, presenting more pits and pores. The retrogradation quality such as SV, relative crystallinity, ΔH_g and ΔH_r were all reduced, and the transmittance range of typical absorption peaks in the FT-IR results were also widened, mainly due to the impaired double helices formation of BRS. Furthermore, *Gl*IRE treatments could effectively improve the texture and flavor of BR. Overall, this paper provides a theoretical basis for the inhibition of starch

retrogradation and quality improvement of BR, offering basic data for the manufacturing of high-quality brown rice products.

CRediT authorship contribution statement

Meilin Cui: Project administration, Writing – review & editing, Funding acquisition, Supervision. **Keke Qiu:** Writing – original draft, Data curation. **Yuchang Ma:** Methodology, Data curation, Conceptualization. **Jiali Wang:** Conceptualization. **Wei Zhao:** Formal analysis, Software. **Xiuhong Zhang:** Supervision.

Declaration of competing interest

The authors declare that they have no known competing financial interests or personal relationships that could have appeared to influence the work reported in this paper.

Acknowledgments

This study was supported by the Applied Basic Research Program of Shanxi Province (grant number: 202203021221135 and 202103021223255), China.

Appendix A. Supplementary data

Supplementary data to this article can be found online at https://doi.org/10.1016/j.crfs.2024.100927.

Data availability

Data will be made available on request.

References

Boondaeng, A., Keabpimai, J., Trakunjae, C., Vaithanomsat, P., Srichola, P., Niyomvong, N., 2024. Cellulase production under solid-state fermentation by *Aspergillus sp.* IN5: parameter optimization and application. Heliyon 10 (5), e26601. https://doi.org/10.1016/j.heliyon.2024.e26601.

Cai, Q.L., Li, X.P., Ding, X.X., Wang, H.R., Hu, X.Z., 2023. Effects of quercetin and Ca $(OH)_2$ addition on gelatinization and retrogradation properties of Tartary buckwheat starch. Lebensm. Wiss. Technol. 178, 114488. https://doi.org/10.1016/j.lwt.2023.114488.

Cen, Q., Fan, J., Zhang, R., Chen, H.Y., Hui, F.Y., Li, J.M., et al., 2024. Impact of *Ganoderma lucidum* fermentation on the nutritional composition, structural characterization, metabolites, and antioxidant activity of Soybean, sweet potato and Zanthoxylum pericarpium residues. Food Chem. X 21, 101078. https://doi.org/10.1016/j.fochx.2023.101078.

Chang, Q., Zheng, B.D., Zhang, Y., Zeng, H.L., 2021. A comprehensive review of the factors influencing the formation of retrograded starch. Int. J. Biol. Macromol. 186, 163–173. https://doi.org/10.1016/j.ijbiomac.2021.07.050.

Chen, C.S., Jiang, S.Y., Li, M.F., Li, Y., Li, H., Zhao, F., et al., 2021. Effect of high temperature cooking on the quality of rice porridge. Int. J. Agric. Biol. Eng. 14, 247–254. https://doi.org/10.25165/j.ijabe.20211405.6412.

Chen, X.P., Zhang, L., Li, X., Qiao, Y., Zhang, Y.J., Zhao, Y.Q., et al., 2020. Impact of maltogenic α-amylase on the structure of potato starch and its retrogradation properties. Int. J. Biol. Macromol. 145, 325–331. https://doi.org/10.1016/j.ijbiomac.2019.12.098.

Chen, Z.G., Yang, Q., Yang, Y.S., Zhong, H.X., 2023. The effects of high-pressure treatment on the structure, physicochemical properties and digestive property of starch - a review. Int. J. Biol. Macromol. 244, 125376. https://doi.org/10.1016/j.ijbiomac.2023.125376.

Cheng, W., Sun, Y.J., Xia, X.Z., Yang, L.Z., Fan, M.C., Li, Y., et al., 2022. Effects of β-amylase treatment conditions on the gelatinization and retrogradation characteristics of wheat starch. Food Hydrocolloids 124, 107286. https://doi.org/10.1016/j.foodhyd.2021.107286.

Cui, M.L., Ma, Y.C., Yu, Y.W., 2021. Heme oxygenase-1/carbon monoxide signaling participates in the accumulation of triterpenoids of *Ganoderma lucidum*. J. Zhejiang Univ. - Sci. B 22 (11), 941–953. https://doi.org/10.1631/jzus.B2000818.

Cui, Y.L., Li, X.T., Sun, D.Y., Guo, L., Cui, B., Zou, F.X., et al., 2024. Retrogradation inhibition of starches in staple foods with maltotetraose-forming amylase. Food Chem. 449, 139232. https://doi.org/10.1016/j.foodchem.2024.139232.

Ghasemi, E., Mosavian, M.T.H., Khodaparast, M.H.H., 2009. Effect of stewing in cooking step on textural and morphological properties of cooked rice. Rice Sci. 16 (3), 243–246. https://doi.org/10.1016/S1672-6308(08)60086-4.

Guan, L., Zhang, M., 2022. Formation and release of cooked rice aroma. J. Cereal. Sci. 107, 103523. https://doi.org/10.1016/j.jcs.2022.103523.

Guo, L., 2018. Sweet potato starch modified by branching enzyme, β-amylase and transglucosidase. Food Hydrocolloids 83, 182–189. https://doi.org/10.1016/j.foodhyd.2018.05.005.

Hu, S.S., Zhu, Q.Y., Ren, A., Ge, L.G., He, J., Zhao, M.W., et al., 2022. Roles of water in improved production of mycelial biomass and lignocellulose-degrading enzymes by water-supply solid-state fermentation of *Ganoderma lucidum*. J. Biosci. Bioeng. 133 (2), 126–132. https://doi.org/10.1016/j.jbiosc.2021.10.006.

Hu, Y., He, C.X., Zhang, M.Y., Zhang, L.Q., Xiong, H., Zhao, Q., 2020. Inhibition from whey protein hydrolysate on the retrogradation of gelatinized rice starch. Food Hydrocolloids 108, 105840. https://doi.org/10.1016/j.foodhyd.2020.105840.

Huang, S.Q., Chao, C., Yu, J.L., Copeland, L., Wang, S.J., 2021. New insight into starch retrogradation: the effect of short-range molecular order in gelatinized starch. Food Hydrocolloids 120, 106921. https://doi.org/10.1016/j.foodhyd.2021.106921.

Jo, M., Qi, J., Du, Z.J., Li, Y.H., Shi, Y.C., 2024. Changes in the structure and enzyme binding of starches during in vitro enzymatic hydrolysis using mammalian mucosal enzyme mixtures. Carbohydr. Polym. 335, 122070. https://doi.org/10.1016/j.carbpol.2024.122070.

Karim, M.D., Abuhena, M., Hossain, M.D., Billah, M.M., 2024. Assessment and comparison of cooking qualities and physio-chemical properties of seven rice varieties in terms of amylose content. Food Physics 1, 100014. https://doi.org/10.1016/j.foodp.2024.100014.

Lan, G.W., Xie, S.M., Duan, Q.F., Huang, W.J., Huang, W., Zhou, J.F., et al., 2024. Effect of soybean polysaccharide and soybean oil on gelatinization and retrogradation properties of corn starch. Int. J. Biol. Macromol. 264, 130772. https://doi.org/10.1016/j.ijbiomac.2024.130772.

Li, D., Fei, T., Wang, Y., Zhao, Y.K., Dai, L.Y., Fu, X.X., et al., 2020. A cold-active 1,4-α-glucan branching enzyme from Bifidobacterium longum reduces the retrogradation and enhances the slow digestibility of wheat starch. Food Chem. 324, 126855. https://doi.org/10.1016/j.foodchem.2020.126855.

Li, J.H., Yuan, Y.H., Zhang, H.X., Zou, F.X., Tao, H.T., Wang, N., et al., 2022. Structural, physicochemical and long-term retrogradation properties of wheat starch treated using transglucosidase. Food Chem. 380, 132226. https://doi.org/10.1016/j.foodchem.2022.132226.

Li, J.H., Zou, F.X., Gui, Y.F., Guo, L., Wang, N., Liu, P.F., et al., 2021. Long-term retrogradation properties of rice starch modified with transglucosidase. Food Hydrocolloids 121, 107053. https://doi.org/10.1016/j.foodhyd.2021.107053.

Li, W.W., Li, C.M., Gu, Z.B., Qiu, Y.J., Cheng, L., Hong, Y., et al., 2016. Retrogradation behavior of corn starch treated with 1,4-α-glucan branching enzyme. Food Chem. 203, 308–313. https://doi.org/10.1016/j.foodchem.2016.02.059.

Li, X.X., Zhai, Y.T., Jin, Z.Y., Bai, Y.X., 2023a. Regulation of multi-scale structures and retrogradation property of A- and B-type wheat starch granules with maltogenic α-amylase. Int. J. Biol. Macromol. 248, 125846. https://doi.org/10.1016/j.ijbiomac.2023.125846.

Li, Z.H., Sun, X.Y., Xu, T., Dai, W., Yan, Q., Li, P., et al., 2023b. Insight into the dynamic variation and retention of major aroma volatile compounds during the milling of Suxiang japonica rice. Food Chem. 405, 134468. https://doi.org/10.1016/j.foodchem.2022.134468.

Liang, Z.L., Chen, X., Luo, J.W., Zhao, H.B., Yang, Z., Zhu, J., 2020. Addition of amino acids to modulate structural, physicochemical, and digestive properties of corn starch-amino acid complexes under hydrothermal treatment. Int. J. Biol. Macromol. 160, 741–749. https://doi.org/10.1016/j.ijbiomac.2020.05.238.

Liu, L.P., Yang, M.N., Wang, L.L., Xu, J., Wang, Q., Fan, X.R., et al., 2019a. Effect of pullulan on molecular chain conformations in the process of starch retrogradation condensed matter. Int. J. Biol. Macromol. 138, 736–743. https://doi.org/10.1016/j.ijbiomac.2019.07.118.

Liu, Q.Z., Chen, P.F., Li, P., Zhao, J., Olnood, C.G., Zhao, S., et al., 2023a. Effects of Salecan on the gelatinization and retrogradation behaviors of wheat starch. Lebensm. Wiss. Technol. 186, 115238. https://doi.org/10.1016/j.lwt.2023.115238.

Liu, X.Y., Guo, Y.B., Wang, S.C., Wang, X.Y., Wang, Z.H., Wang, Z., 2024. Effects of ultrasound combined with hydrothermal treatment on the quality of brown rice. Lebensm. Wiss. Technol. 196, 115874. https://doi.org/10.1016/j.lwt.2024.115874.

Liu, Y.F., Chen, J., Wu, J.Y., Luo, S.J., Chen, R.Y., Liu, C.M., et al., 2019b. Modification of retrogradation property of rice starch by improved extrusion cooking technology. Carbohydr. Polym. 213, 192–198. https://doi.org/10.1016/j.carbpol.2019.02.089.

Liu, Z.Y., Zhong, Y.Y., Khakimov, B., Fu, Y.X., Pawel Czaja, T., Judas Kain Kirkensgaard, J., et al., 2023b. Insights into high hydrostatic pressure pre-treatment generating a more efficient catalytic mode of maltogenic α-amylase: effect of multi-level structure on retrogradation properties of maize starch. Food Hydrocolloids 138, 108480. https://doi.org/10.1016/j.foodhyd.2023.108480.

Luo, X.Y., Li, D.D., Tao, Y., Wang, P., Yang, R.Q., Han, Y., 2022. Effect of static magnetic field treatment on the germination of brown rice: changes in α-amylase activity and structural and functional properties in starch. Food Chem. 383, 132392. https://doi.org/10.1016/j.foodchem.2022.132392.

Manavalan, T., Manavalan, A., Thangavelu, K.P., Heese, K., 2015. Characterization of a novel endoglucanase from *Ganoderma lucidum*. J. Basic Microbiol. 55 (6), 761–771. https://doi.org/10.1002/jobm.201400808.

Meng, N., Kang, Z.Y., Jiang, P., Liu, Y.X., Liu, M., Li, Q.Y., 2024. Effects of fucoidan and ferulic acid on potato starch: pasting, rheological and retrogradation properties and their interactions. Food Hydrocolloids 150, 109635. https://doi.org/10.1016/j.foodhyd.2023.109635.

Niu, L.Y., Wu, L.Y., Xiao, J.H., 2017. Inhibition of gelatinized rice starch retrogradation by rice bran protein hydrolysates. Carbohydr. Polym. 175, 311–319. https://doi.org/10.1016/j.carbpol.2017.07.070.

Oh, S.M., Kim, H.Y., Bae, J.E., Ye, S.J., Kim, B.Y., Choi, H.D., et al., 2019. Physicochemical and retrogradation properties of modified chestnut starches. Food Sci. Biotechnol. 28, 1723–1731. https://doi.org/10.1007/s10068-019-00622-8.

Peng, Q., Meng, K., Zheng, H.J., Yu, H.F., Zhang, Y.H., Yang, X.Y., et al., 2022. Metabolites comparison in post-fermentation stage of manual (mechanized) Chinese Huangjiu (yellow rice wine) based on GC–MS metabolomics. Food Chem. X 14, 100324. https://doi.org/10.1016/j.fochx.2022.100324.

Rolandelli, G., Rodríguez, S.D., Buera, M.d.P., 2024. Modulation of the retrogradation kinetics of sweet potato starch by the addition of pectin, guar gum, and gallic acid. Food Hydrocolloids 146, 109211. https://doi.org/10.1016/j.foodhyd.2023.109211.

Rostamabadi, H., Yildirim-Yalcin, M., Demirkesen, I., Toker, O.S., Colussi, R., do Nascimento, L.Á., et al., 2024. Improving physicochemical and nutritional attributes of rice starch through green modification techniques. Food Chem. 458, 140212. https://doi.org/10.1016/j.foodchem.2024.140212.

Sansenya, S., Hua, Y.L., Chumanee, S., 2018. The correlation between 2-Acetyl-1-pyrroline content, biological compounds and molecular characterization to the aroma intensities of Thai local rice. J. Oleo Sci. 67 (7), 893–904. https://doi.org/10.5650/jos.ess17238.

Shah, A., Masoodi, F.A., Gani, A., Ashwar, B., 2017. Physicochemical, rheological and structural characterization of acetylated oat starches. LWT - Food Sci. Technol. 80, 19–26. https://doi.org/10.1016/j.lwt.2017.01.072.

Shah, A., Masoodi, F.A., Gani, A., Ashwar, B., 2018. Dual enzyme modified oat starch: structural characterisation, rheological properties, and digestibility in simulated GI tract. Int. J. Biol. Macromol. 106, 140–147. https://doi.org/10.1016/j.ijbiomac.2017.08.013.

Shi, M.M., Zhang, Z.H., Yu, S.J., Wang, K., Gilbert, R.G., Gao, Q.Y., 2014. Pea starch (*Pisum sativum* L.) with slow digestion property produced using β-amylase and transglucosidase. Food Chem. 164, 317–323. https://doi.org/10.1016/j.foodchem.2014.05.045.

Surendran, A., Siddiqui, Y., Ali, N.S., Manickam, S., 2018. Inhibition and kinetic studies of cellulose- and hemicellulose-degrading enzymes of Ganoderma boninense by naturally occurring phenolic compounds. J. Appl. Microbiol. 124 (6), 1544–1555. https://doi.org/10.1111/jam.13717.

Vajravijayan, S., Pletnev, S., Mani, N., Pletneva, N., Nandhagopal, N., Gunasekaran, K., 2018. Structural insights on starch hydrolysis by plant β-amylase and its evolutionary relationship with bacterial enzymes. Int. J. Biol. Macromol. 113, 329–337. https://doi.org/10.1016/j.ijbiomac.2018.02.138.

Villas-Boas, F., Franco, C.M.L., 2016. Effect of bacterial β-amylase and fungal α-amylase on the digestibility and structural characteristics of potato and arrowroot starches. Food Hydrocolloids 52, 795–803. https://doi.org/10.1016/j.foodhyd.2015.08.024.

Wan, L.Y., Wang, X.D., Liu, H.Y., Xiao, S.S., Ding, W.P., Pan, X.Y., et al., 2023. Retrogradation inhibition of wheat starch with wheat oligopeptides. Food Chem. 427, 136723. https://doi.org/10.1016/j.foodchem.2023.136723.

Wang, H.W., Xiao, N.Y., Ding, J.T., Zhang, Y.Y., Liu, X.L., Zhang, H., 2020. Effect of germination temperature on hierarchical structures of starch from brown rice and their relation to pasting properties. Int. J. Biol. Macromol. 147, 965–972. https://doi.org/10.1016/j.ijbiomac.2019.10.063.

Wang, J.Y., Jiang, X.F., Guo, Z.B., Zheng, B.D., Zhang, Y., 2021. Long-term retrogradation behavior of lotus seed starch-chlorogenic acid mixtures after microwave treatment. Food Hydrocolloids 121, 106994. https://doi.org/10.1016/j.foodhyd.2021.106994.

Wang, S.J., Li, C.L., Copeland, L., Niu, Q., Wang, S., 2015. Starch retrogradation: a comprehensive review. Compr. Rev. Food Sci. Food Saf. 14, 568–585. https://doi.org/10.1111/1541-4337.12143.

Wang, S.H., Tian, A.L., Zhao, K., Zhang, R., Lei, Z.X., Qin, X.H., et al., 2023. Effect of cooking methods on volatile compounds and texture properties in rice porridge. Lebensm. Wiss. Technol. 184, 115111. https://doi.org/10.1016/j.lwt.2023.115111.

Wu, C.S., Zhou, X., Tian, Y.Q., Xu, X.M., Jin, Z.Y., 2017. Hydrolytic mechanism of α-maltotriohydrolase on waxy maize starch and retrogradation properties of the hydrolysates. Food Hydrocolloids 66, 136–143. https://doi.org/10.1016/j.foodhyd.2016.12.016.

Wu, S.J., Zhang, S.Y., Peng, B., Tan, D.C., Wu, M.Y., Wei, J.C., et al., 2024. *Ganoderma lucidum:* a comprehensive review of phytochemistry, efficacy, safety and clinical study. Food Sci. Hum. Wellness 13 (2), 568–596. https://doi.org/10.26599/FSHW.2022.9250051.

Xiong, R.Y., Tan, X.M., Yang, T.T., Pan, X.H., Zeng, Y.J., Huang, S., et al., 2022a. Relation of cooked rice texture to starch structure and physicochemical properties under different nitrogen managements. Carbohydr. Polym. 295, 119882. https://doi.org/10.1016/j.carbpol.2022.119882.

Xiong, Y., Zhang, F.L., Li, J.R., Peng, P.Z., Liu, B., Zhao, L.N., 2022b. *Ganoderma lucidum* protease hydrolyzate on lipid metabolism and gut microbiota in high-fat diet fed rats. Food Biosci. 47, 101460. https://doi.org/10.1016/j.fbio.2021.101460.

Yan, W.J., Yin, L.J., Zhang, M.H., Zhang, M., Jia, X., 2021. Gelatinization, retrogradation and gel properties of wheat starch–wheat bran arabinoxylan complexes. Gels 7 (4), 200. https://doi.org/10.3390/gels7040200.

Ye, J.P., Liu, C.M., Luo, S.J., Hu, X.T., McClements, D.J., 2018. Modification of the digestibility of extruded rice starch by enzyme treatment (β-amylolysis): an in vitro study. Food Res. Int. 111, 590–596. https://doi.org/10.1016/j.foodres.2018.06.002.

Zeng, X.X., Zheng, B., Xiao, G.S., Chen, L., 2022. Synergistic effect of extrusion and polyphenol molecular interaction on the short/long-term retrogradation properties of chestnut starch. Carbohydr. Polym. 276, 118731. https://doi.org/10.1016/j.carbpol.2021.118731.

Zhai, Y.T., Li, X.X., Bai, Y.X., Jin, Z.Y., Svensson, B., 2022. Maltogenic α-amylase hydrolysis of wheat starch granules: mechanism and relation to starch retrogradation. Food Hydrocolloids 124, 107256. https://doi.org/10.1016/j.foodhyd.2021.107256.

Zhang, R., Cen, Q., Hu, W.K., Chen, H.Y., Hui, F.Y., Li, J.M., et al., 2024. Metabolite profiling, antioxidant and anti-glycemic activities of Tartary buckwheat processed by solid-state fermentation(SSF)with *Ganoderma lucidum*. Food Chem. X 22, 101376. https://doi.org/10.1016/j.fochx.2024.101376.

Zhang, Z.W., Ying, Y.N., Zhang, L., Dai, G.X., Deng, G.F., Bao, J.S., et al., 2023. Starch structural reasons for the effects of SSIIIa deficiency on the textural and digestive properties of cooked rice. J. Cereal. Sci. 111, 103671. https://doi.org/10.1016/j.jcs.2023.103671.

Zhao, Q.Y., Xi, J.Z., Xu, D., Jin, Y.M., Wu, F.F., Tong, Q.Y., et al., 2022. A comparative HS-SPME/GC-MS-based metabolomics approach for discriminating selected japonica rice varieties from different regions of China in raw and cooked form. Food Chem. 385, 132701. https://doi.org/10.1016/j.foodchem.2022.132701.

Zhao, W.Q., Liang, W., Ospankulova, G., Muratkhan, M., Kh, K.Z., Li, W.H., 2023. Electron beam irradiation modification of ultra-high pressure treated broad bean starch: improvement of multi-scale structure and functional properties. Food Chem. 427, 136690. https://doi.org/10.1016/j.foodchem.2023.136690.